Peer-reviewed version available at energies 2019, 12, 1385; doi:10.3390/en12071385

Two-Layer Routing for High-Voltage Powerline Inspection by Cooperated Ground Vehicle and Drone

Yao Liu[1], Jianmai Shi[1,*], Zhong Liu[1], Jincai Huang[1], Tianren Zhou[1]

[1]*Science and Technology on Information Systems Engineering Laboratory, College of System Engineering, National University of Defense Technology, Changsha, 410073, P. R. China.*

[*]*Corresponding author: jianmaishi@gamil.com.*

Abstract

A novel high-voltage powerline inspection system is investigated, which consists of the cooperated ground vehicle and drone. The ground vehicle acts as a mobile platform that can launch and recycle the drone, while the drone can fly over the powerline for inspection within limited endurance. This inspection system enables the drone to inspect powerline networks in a very large area. Both vehicle' route in the road network and drone's routes along the powerline network have to be optimized for improving the inspection efficiency, which generates a new two-layer point-arc routing problem. Two constructive heuristics are designed based on "Cluster First, Rank Second" and "Rank First, Split Second". Then local search strategies are developed to further improve the quality of the solution. To test the performance of the proposed algorithms, practical cases with different-scale are designed based on the road network and powerline network of Ji'an, China. Sensitivity analysis on the parameters related with the drone's inspection speed and battery capacity is conducted. Computational results indicate that technical improvement on the inspection sensor is more important for the cooperated ground vehicle and drone system.

Keywords: high-voltage powerline inspection; vehicle routing; arc routing; drone; heuristic

1. Introduction

Economic expansion and development of urbanization have led to an enormous increase in demand for electricity consumption, requiring the high reliability of the power supply. As the connection between the electricity generation node and customer nodes, high-voltage power transmission lines act as an important role in the overall performance of the electrical network. Most powerlines are far away from main roads and household centers for considerations of safety, environment protection, as well as construction and transmission cost saving. Traditionally, the inspection of high-voltage powerlines is mainly conducted by manned helicopters or foot patrol, which is inefficient and expensive, sometimes even presents heavy workload and unknown dangers for inspection technicians. When powerlines cross forest, rivers or other geographic circumstances unreachable for manual inspection, this work becomes much more difficult. Thus, it is one of the most important work in power management for finding more effective and economic ways to inspect powerlines.

In recent years, drone-assisted powerline inspection has been identified as a viable alternative way, due to the rapid development of automation and artificial intelligence technologies [1, 2]. The advent of airborne sensors, such as thermal infrared imager and visible light camera, allows the drone to detect common faults, including transmission line fault, loss of line equipment and damage of transmission tower. Without the limitation of road distribution and geographical issue, the drone is free of collisions and obstacles, and realizes the autonomous inspection along the powerlines, which can significantly reduce the time and capital cost of the inspection. Furthermore, there is no risk of casualties for technicians, as they do not need to directly face the complex environment or perform dangerous operations. Given these advantages, many companies have tried to apply drone for powerline inspection. In November, 2018, Ameren successfully utilized a drone for a 60-mile transmission line inspection [3]. Another company in America, Indiana Michigan Power (I&M), has achieved drone inspection on transmission lines in Randolph County since January, 2019 [4]. In china, more and more enterprises in power industry apply drones for powerline inspection [5]. Intelligent inspection systems are developed on the small drone equipped with HD camera and infrared thermal imager, which has been successfully applied on 500kV and 220kV powerlines in some provinces, such as Shandong and Gansu.

However, there are some obstacles that prevents the wide adoption of the drone-assisted powerline inspection. Sometimes, the drone needs to be employed for closer inspection and fly at low altitude or hover in some crucial areas, which means small-scale drones are more versatile for accurate detection. But with limited endurance, small drones are difficult to inspect in long distance and for a long time. For most drones, their capacities of battery power are not sufficient for long-term inspection mission. Second, the establishing cost for the control and communication center is too expensive, and it is

Preprints (www.preprints.org) | NOT PEER-REVIEWED | Posted: 7 February 2019 doi:10.20944/preprints201902.0072.v1

Peer-reviewed version available at energies 2019, 12, 1385; doi:10.3390/en12071385

unpractical to construct many ground base stations in the powerline network. Furthermore, it would cause the failure of communications as well as much waste of time and energy when the drone leaves the station to inspect powerlines too far away. To overcome these practical difficulties, a cooperated Ground Vehicle (GV) and drone system for powerline inspection is presented in Figure 1, which introduces a novel powerline inspection mode.

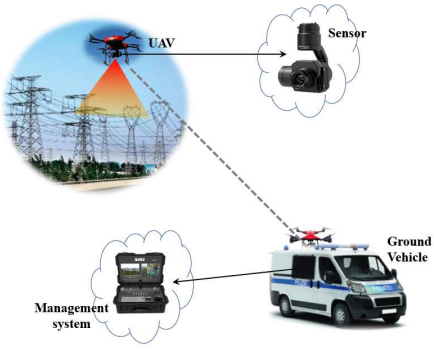

Figure 1. Illustration of powerline inspection by the cooperated ground vehicle and drone system

The powerline inspecting system is formed by the cooperated ground vehicle and drone. Equipped with the control and communication system, the ground vehicle serves as a mobile base station. The ground vehicle can drive to a location near the powerline in the road network and then launch the drone. When the drone inspects with airborne sensors along the powerline, the technicians on the vehicle can control the flight of drone and process the data and images captured by the drone. Simultaneously, the ground vehicle keeps moving forward to the next rendezvous close to the powerline and recycle the drone before it runs out of its energy. The operations for charging or replacing the battery of the drone can be conducted on the vehicle, and then the drone can rapidly go on the inspection again. This new mode has several notable advantages. Initially, acting as the moving station, the ground vehicle can offset the drone's disadvantage on limited endurance and enable the drone to inspect powerlines in a very large area. Second, the ground vehicle can move forward to pick up the drone, which shortens the drone's flight distance and greatly improve the inspection efficiency. Thirdly, with shorter distance between the vehicle and the drone, communications are more stable, which facilitates the effective control of the drone and timely analysis of the collected data.

Although the new powerline inspection mode by cooperated vehicle and drone is efficient both in time and cost, it brings many new challenges on the route planning of the vehicle and drone. As displayed in Figure 2, the vehicle travels on the road network while the drone flies along the high-voltage power transmission line, which causes a novel two-layer point-arc routing problem (2L-PA-RP). The road network for the ground vehicle is in the lower layer, where there are a set of potential parking nodes for launching and recycling the drone. The network of the high-voltage powerlines is in the upper layer. The drone is launched from the vehicle at a parking node, flies to the powerline, conducts inspections along the line and then returns to the vehicle at another parking node before the battery powers off. The routing planning for the vehicle and the drone is to optimize the locations (parking nodes) for launching/recycling the drone, vehicle's route on the road network for visiting these nodes, and drone's routes on the powerline network, so as to minimize the completion time or the cost for inspecting all the powerlines. The 2L-PA-RP integrates two classical routing problems, the Travelling Salesman Problem with visiting node selection (the lower layer subproblem) and the arc routing problem (the upper layer subproblem), both of which are NP-Hard. Besides, the interaction between the two layers has to be considered, that is the drone must frequently departure from or return to the ground vehicle during the inspection process. Thus, the ground vehicle's route and moving should cooperate with the drone's routes and flying in both spatial and temporal domains, which makes the problem much more complex and difficult to solve.

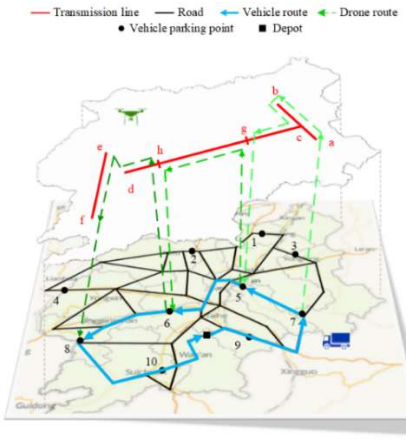

Figure 2. Illustration of the two-layer point-arc routing problem

Motivated by the adaption of new technologies and inspection tool (drone) in power delivery industry, a novel two-layer point-arc routing problem for the cooperated GV and drone is investigated. Due to the complexity of the problem, efficient heuristics are designed to solve it. Three practical instances with different sizes are illustrated based on powerline network and road network in Ji'an, a city in China, which are used to test the performance of the solution approaches. Sensitivity analysis for critical parameters is conducted for finding their influence on the efficiency of the novel cooperated inspection system.

The paper is structured as follows. Section 2 presents the literature review, and Section 3 illustrates the problem and the model. Section 4 introduces the heuristic algorithms. The experiment with three actual cases is conducted in Section 5. At last, Section 6 presents the conclusion and future works.

2. Literature Review

Electricity production and distribution has been always the area of immense concern. Nowadays, with rapid increase of energy demand, many researchers have made a great contribution to the planning and expansion of power system [6-9]. Sarıca et al. [10] even developed a model to investigate the implications of the power market on profits, prices, availability and supply security, which also entails a critical challenge to power transmission line inspection.

It is an important research topic for researchers to find more economical and efficient ways for power system inspection. In 1991, Tokyo electric power Company proposed a mobile robot for detecting the 66KV fiber-optic overhead ground wires (OPGW), which can run on the OPGW and negotiate obstacles such as counterweights and clamp [11]. Since then, many studies discussed the hardware design and software construction of the inspection robot. Most of these researches focused on the obstacle avoidance of the inspection robot, such as Zhou [12] and Zhu [13]. In 2009, Katrasnik et al. [14] conducted a survey on the mobile robots applied in transmission line inspection and discussed the inspection with automated helicopter or flying robots. Besides, the corresponding software design, like database environment [15] and feature matching of detecting images [16], were also studied.

With the development of remote sensing and artificial intelligence technology, the drone presents huge application opportunities after 2010. Due to the high efficiency and low cost, drone plays an important role on the inspection of bridge, cell towers and so on [17, 18]. In electricity field, the drone has been applied on the inspection for both transmission structure [19] and powerline [20]. And various inspection systems are developed based on different kinds of drones. Hrabar et al. [21] developed a platform of autonomous small helicopter and showed that both fixed-wing and rotorcraft UAVs (RUAVs) are suitable for powerline inspection. It was also proved that RUAVs are more versatile with the ability of hovering and vertical climbing or descending. A similar work was also carried out by Luque-Vega et al. [22], which is based on the quad-rotor helicopter. They even conducted some experiment on the electrical network of Mexico to demonstrate the feasibility of the proposed system. Additionally, Huang et al. [23] focused on the fixed-wing UAV and realized the low-speed low-altitude patrol in suspected locations. There were a very few researches mentioned large unmanned helicopter, which can schedule multiple sensors to track the power lines automatically [24]. Pirbodaghi, et al. [25] designed a cooperative heterogeneous unmanned autonomous system, in which a three-arms robot moves on the transmission lines while a drone inspects the transmission tower.

In order to ensure the accuracy of drone inspection, some algorithms were proposed. Primarily, a variety of classification and recognition algorithms were designed as the drone inspection is based on the images captured by the airborne camera [26-30]. The supervised learning approach and network training method were applied in the classification problem of inspection images [26, 28]. The decomposition algorithm is used to distinguish the transmission line from the natural outdoor environment [27] or eliminate the influence of flog weather [30]. Furthermore, a cloud-based architecture was established to enable real-time video streaming and facilitate communications [31]. There is also a research on the risk assessment of the drone in the powerline inspection process [32].

In the overall works mentioned above, we can see that almost of the studies are concerned about the hardware design or the flight control for drone inspection. There are only two papers discussing the route planning in the inspection problem with drone. One is proposed in 2009, involving the mission planning of the flying robot for powerline inspection [33]. It developed a basic planning system to directly give the inspection scheme, including checking order, space path and flight trajectory. Since it mainly focused on the robot control, it did not pay much attention on the optimization of path planning. The other research studied the drone inspection for electric transmission towers [34]. Three performance ratios were considered in the optimization, including flight time, image quality, and tower coverage. A particle swarm optimization (PSO) based algorithm and a simulated annealing (SA) based algorithm were designed to solve the problem. With only transmission towers involved and without transmission lines, the problem was modeled as a Traveling Salesman Problem.

From the above review, the inspection problem of power transmission line with cooperated ground vehicle and drone has not been studied, which is a novel system and can be employed for powerline inspection. The newly generated two-layer point-arc routing problem for the cooperated ground vehicle and drone is important for efficiently utilizing this novel system, which has not been investigated. Therefore, this paper studies this new problem and develops an efficient approach to optimize the routes for both the ground vehicle and drone.

3. Problem Description and Model Development

3.1 Problem description

In the two-layer point-arc routing problem (2L-PA-RP), the vehicle travels on the road network while the drone flies along the transmission line. Ground vehicle can only stop at the predefined parking nodes. And the endurance capacity of the drone is limited and known. The problem aims to optimize both drone routes on the powerline network and vehicle routes on the road network, involving the selection of parking locations, so as to minimize the completion time for the whole powerline inspection task.

Preprints (www.preprints.org) | NOT PEER-REVIEWED | Posted: 7 February 2019 doi:10.20944/preprints201902.0072.v1

Peer-reviewed version available at energies 2019, 12, 1385; doi:10.3390/en12071385

Figure 3 shows the aerial view of the example 2L-PARP in Figure 2, which contains 4 powerline arcs (<a, c>, <b, c>, <c, d>, <e, f>) and 10 potential parking nodes. It can be seen that the arc <e, f> is not connected with other arcs, and this situation appears when segments represent powerlines of different voltages. The route traveled by the ground vehicle is the lower layer, represented as blue solid lines, whereas the drone routes, depicted as green dashed lines, belong to the upper layer.

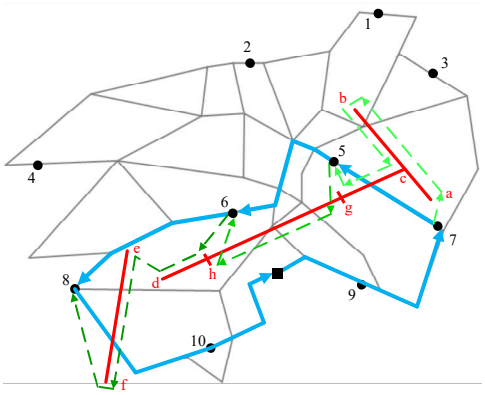

Figure 3. Aerial view of a solution for the example in Figure 2

More formally, the 2L-PA-RP can be described as follows. Two undirected graphs are defined, which are $G_G = (V_G, E_G)$ for the road network and $G_D = (V_D, E_D)$ for the powerline network. Set V_G is the set of all parking nodes and V_D is the set of all the vertices in the powerline network. Set E_G is the set of edges on the road network while E_D contains the edges that can be traveled by the drone.

Specifically, the ground vehicle can travel with the speed of v_g only on the edges in E_G, which are all located in the lower layer. Each edge $e_g \in E_G$ can be represented by $< i, j > (i, j \in V_G)$, and its distance can be calculated as d_{ij}^1, which is not the Euler distance but the actual travelling distance for the ground vehicle on the road network.

As for the upper layer, let $E_R \subset E_D$ be the set of edges required to be inspected, which is {<a, c>, <b, c>, <c, d>, <e, f>} in Figure 3. Represented by $< i, j > (i, j \in V_D)$, the linear distance of any required edge $e_r \in E_R$ can be calculated as d_{ij}^2, and the edge is said to be served if and only if the drone traverses the arc for one time. Since the drone can fly into or out of the powerline at any node, each edge $e_r \in E_R$ can be served in one flight or several flights. For instance, Edge <a, c> and <b, c> is only included in one drone route while Edge <c, d> is divided into three segments, which are <c, g> inspected in the first flight, <g, h> inspected in the second flight and <h, d> inspected in the third flight. In the drone route, there are two kinds of flight, regular flight and inspection flight. The drone can fly quickly from the vehicle to the node on the transmission line (e.g. 7→a) or from one powerline node to another (e.g. b→c), and inspect the powerline with airborne sensors at a slow speed (e.g. a → b). We respectively denote the inspection speed as v_d^1 and the regular flight speed as v_d^2 ($v_d^1 \le v_d^2$). Besides, the airborne sensors would not work and stay in standby state when the drone is in regular flight. Thus, the power consumption rate of the drone per unit time during inspection, denoted as p^1, is assumed to be higher than that during regular flight, p^2 ($p^1 > p^2$). The more detailed calculation for the energy consumption process of the drone is presented in section 3.2.

To represent the powerline segments, we introduce a variable λ^{ij}_m into the edge $< i, j > (i, j \in V_D)$, represent node m on the edge, among which

$$\lambda_m^{ij} = \frac{d_{im}^1}{d_{ij}^1} (0 < \lambda_m^{ij} < 1) . \quad (1)$$

For instance, the node g can be described as $\lambda_g^{cd} = d_{cg}^1 / d_{cd}^1$. Thus, each drone flight route can be encoded as an order list s, in which the first number is the departure road node, the last number is the returning road node, and the middle numbers represent the inspection powerline segments, such as s_1: {7, a, c, b, c, g, 5}, s_2:{5, g, h, 6} and s_3:{6, h, e, f, 8} in Figure 3.

Since the ground vehicle must arrives at the end node before the drone, thus the drone would spend more time on the flight s_k than the vehicle travelling from the start node to the end node. Let $t_1(s_k)$ denote the time that the drone finishes the drone flight s_k, which also means the completing time for the corresponding sub-solution. In some situations, flight s_k is not connected with flight s_{k+1}, and the ground vehicle have to recycle the drone at the end node of s_k and carry the drone to the start node of s_{k+1} to launch it. Let $t_2(s_k, s_{k+1})$ denote the time that the vehicle travel from the end node of sub-solution s_k to the start node of sub-solution s_{k+1}.

A feasible solution for 2L-PA-RP should satisfy the following constraints:

- All the edges of the powerline network must be inspected by the drone, and each edge is visited for only once.
- The ground vehicle should start at the deport and return to the deport at end.
- The ground vehicle has to arrive at the parking node before the drone so as to recycle it in time.
- The drone must return to the truck before its battery is power off.
- The route of the ground vehicle must be successive.
- Each route of the drone must be successive.

The total time of a feasible solution for completing the inspection task can be calculated as follows.

$$f(S) = \sum_{s_k \in S} t_1(s_k) + \sum_{s_k \in S} t_2(s_k, s_{k+1}) \quad (2)$$

where S is the set of all drone's routes. In function (2) the launching and recycling time of the drone is neglected.

The objective of 2L-PA-RP is to find the feasible solution that minimizes the time for completing the

inspection of the powerline network.

3.2 Energy consumption model of the drone

When the drone flies from the ground vehicle to the transmission line, or from one transmission line to another, the airborne sensors would stay in the standby state, which can save more energy than that during the inspection. In one drone flight, the inspection time is denoted as t^1, and the regular flight time is t^2. With the maximum capacity of the drone battery, D, the energy consumption in one drone route must satisfy the constraint:

$$p^1 t^1 + p^2 t^2 \le D. \tag{3}$$

Since the weight of payload would not be change during the task, we assume that the total weigh of the drone with its airborne sensors is G. The flying speed for powerline inspection is denoted as v_d^1 and the flying speed under regular state is denoted as v_d^2. According to D'Andrea [35], the powers power consumption rate of the drone per unit time under different states can be respectively calculated as follows.

$$p^1 = \frac{G v_d^1}{370\eta\gamma} + e, \tag{4}$$

$$p^2 = \frac{G v_d^2}{370\eta\gamma} + p_s + e, \tag{5}$$

where η is the conversion efficiency of the motor, γ is the lift ratio, e is the energy loss of the drone battery, and p_s is the energy consuming rate of the airborne sensors.

Suppose that the drone flies at a constant speed when inspecting the powerline, and let $\varphi = 370\eta\gamma/G$, which can be calculated with the brand and type of the drone. Similarly, the drone keeps constant speed at the regular flight state. Then the constraint (3) can be expressed with inspection distance, d^1, and regular flight distance, d^2, which is

$$\frac{(\varphi v_d^1 + e) d^1}{v_d^1} + \frac{(\varphi v_d^2 + p_s + e) d^2}{v_d^2} \le D. \tag{6}$$

4. Solution Algorithm

As 2L-PA-RP integrates two NP-Hard problem, TSP and ARP, it is difficult to solve the problem in acceptable time, especially for large size instances. Two constructive heuristics are proposed in this section, which can generate a better feasible solution in short time. The first heuristic is designed based on the idea of "Cluster First, Route Second" (CFRS) while the second one employs the idea of "Route First, Split Second" (RFSS). Then some local search strategies are developed to further improve the solution obtained by the heuristics.

4.1 Heuristic based on "Cluster First, Route Second"

The basic idea of " Cluster First, Route Second "is to split the problem into two simpler routing problems: capacitated arc routing problems (CARP) and a variant of traveling salesman problem (TSP). Firstly, all the powerlines would be inspected by constructing a set of drone routes under the limitations of the drone's endurance capacity and the time relationship between the ground vehicle and the drone. Then a cluster function would be applied to merge some drone routes and generate sub-solutions. Finally, the vehicle route is built by connecting all the sub-solutions, which is solved by CW saving algorithm.

4.1.1 Generating sub-solutions

When generating sub-solutions, all the powerlines are firstly divided into multiple segments on the basis of inflection nodes (Line 1), such as four transmission line segments (<a,c>, <c,b>, <c,d> and <e,f>) of the example in Figure 3. Then for each segment, try to construct a complete drone route (Line 3-5). Specifically, the nearest parking node for each endpoint of the segment would be selected as the launching node or the taking-off node (Line 4). If the drone can travel from one nearest road node and return back to the other after inspection without violating the endurance limitation and if the vehicle can recycle the drone immediately when the drone returns (Line 5), a feasible drone route would be constructed for this segment (Line 6). If the two constraints cannot be satisfied, the powerline segment would be divided into two equal parts and replaced with two new segments (Line 8). Repeat these steps until all the powerlines are inspected (Line 3-9). Finally, to improve the utilization of the drone, some drone routes would be merged (Line 11), which would finally form the sub-solutions for the whole inspection task. And the main algorithm is shown in Algorithm 1.

Algorithm 1: Generating sub-solutions	
1	Divide the transmission lines into segments
2	**WHILE** (there exist unvisited line segments) **DO**
3	Select an unvisited line segment
4	Find two nearest road nodes as launching node and taking-off node
5	**IF** drone route can be built without violating the constraints **THEN**
6	Construct the drone route
7	**ELSE**
8	Replace the segment with two new segments
9	**END IF**
10	**END WHILE**
11	Cluster some drone routes and form sub-solutions

Preprints (www.preprints.org) | NOT PEER-REVIEWED | Posted: 7 February 2019 doi:10.20944/preprints201902.0072.v1

Peer-reviewed version available at energies 2019, 12, 1385; doi:10.3390/en12071385

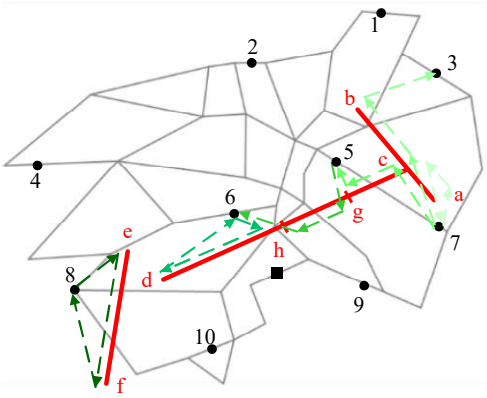

(a) drone routes before merging

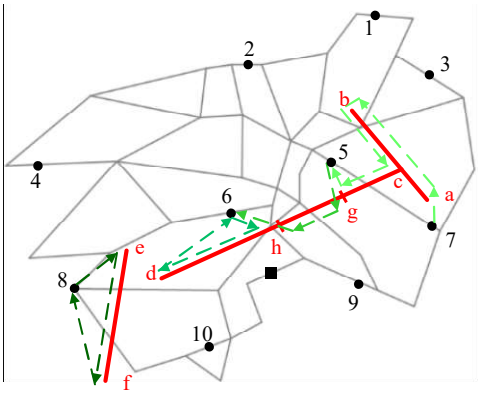

(b) drone routes after merging

Figure 4. An illustration of the drone routes for the example case

Take the case in Figure 3 as an example. For segment <a,c>, node 7 is the nearest parking node for both the endpoint a and c. Thus, after verifying the feasibility, the drone takes off from node 7, enters the power grid from endpoint a, and finally returns to the vehicle from endpoint c to node 7 after completing the inspection of the segment <a,c>. For segment <c,b>, the nearest parking nodes for two endpoints are different, which construct a drone route as {7, c, b, 3}. However, for the segment <c,d>, the distance is too long to complete the inspection by one drone route. Therefore, the midpoint h is inserted to change the old segment <c,d> into two new segments, which are <c,h> and <h,d>. Then the same way of generating drone routes is applied on the two new segments. It goes well for the segment <h,d>, which can be inspected in one flight as {6, h, d, 6}. But for segment <c,h>, after finding nearest parking nodes 7 and 6, the vehicle would spend more time on the travelling from node 7 to 6 than the time that the drone consumes for the flying route, which means the route {7, c, h, 6} cannot satisfy the time relationship between the drone and the vehicle. Thus, two new drone routes {7, c, g, 5} and {5, g, h, 6} are formed. Finally, 6 drone routes are generated for the example case, which is displayed in Figure 4(a).

A merging operation is presented in Algorithm 2 to improve the sub-solutions obtained in Algorithm 1. For each sub-solution, all subsequent sub-solutions are traversed to find whether there exists a sub-solution that can save time through the merging operation (Line 4-8). If the most time-saving sub-solution can be found (Line 9), then conduct the merging operation (Line 10), otherwise stop the cycle (Line 12). Particularly, since in the drone route of this problem, the time cost of forward flight is the same with that of reverse flight, which means the drone route is undirected, thus the forward merging and reverse merging would both be considered in the calculation (Line 6). Figure 4(b) shows the result of the example case after merging. Route {7, a, c, 7}, {7, c, b, 3}, {7, c, g, 5} are merged into a new drone route {7, a, c, b, c, g, 5}.

Algorithm 2: Merging drone routes

```
1   m: the number of drone routes
2   FOR i = 1 to m-1 DO
3       WHILE (1) DO
4           FOR j = i+1 to m DO
5               IF drone route i and drone route j can be merged THEN
6                   Calculate the saving time (i, j)
7               END IF
8           END FOR
9           IF exists a drone route that can save time through merging THEN
10              Merge drone route i with the most saving drone route
11          ELSE
12              Break
13          END IF
14      END WHILE
15  END FOR
```

4.1.2 Constructing vehicle route

After constructing the drone routes, multiple sub-solutions covering the entire power grid are obtained, each of which can be regarded as a target that must be visited by the ground vehicle. But there are two endpoints for each sub-solution. Since drone routes are all undirected, it would cause different results which endpoint the vehicle would choose as the start node. Thus, it can be seen as a variant of traveling salesman problem.

CW Saving algorithm [36], which can provide an effective way for solving the TSP problems, is applied to construct the vehicle route. The main procedure is shown in Algorithm 3.

The sub-solutions generated by Algorithm 2 are set as initial input of Algorithm 3. An array for recording the vehicle route would be declared, in which the first element is initialized as the first sub-solution (Line 2). Then the remaining sub-solutions would be inserted into the array in the labeled order (Line 3). After calculating the added cost for every position that each sub-solution can be inserted into the array (Line 4-6), the position with minimum add cost (time) would be chosen (Line 7). Specifically, there are two ways for the vehicle to visit a sub-solution, depending on which end point would be selected as the

Preprints (www.preprints.org) | NOT PEER-REVIEWED | Posted: 7 February 2019 doi:10.20944/preprints201902.0072.v1

Peer-reviewed version available at energies 2019, 12, 1385; doi:10.3390/en12071385

enter node. For example, the vehicle can visit the {7, a, c, b, c, g, 5} from node 7 while the opposite direction to enter the sub-solution from node 5 is also feasible. Thus, different directions should both be considered when calculating the added cost (time). At last, a vehicle route is constructed.

Algorithm 3: Constructing vehicle route

1 *m*: the number of the generated sub-solutions
2 **INITIALIZE** subsoluArray
3 **FOR** tempSubSolu = 2 to *m* **DO**
4 **FOR** *i* = 1 to length(subsoluArray)+1 **DO**
5 Calculate added cost when putting tempSubSolu into subsoluArray at position *i*
6 **END FOR**
7 Choose the position with minimum add cost to insert tempSubSolu
8 Update the subsoluArray
9 **END FOR**

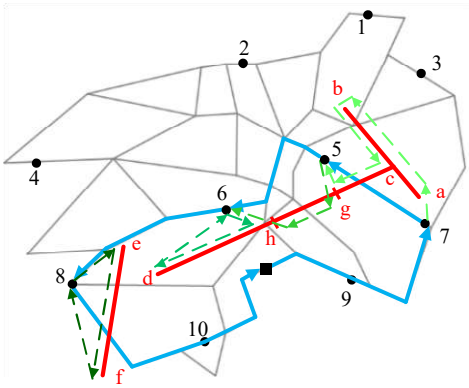

Figure 5. An illustration of the feasible solution by CFRS for the example case

After constructing the drone routes and the vehicle route, an initial feasible solution can be obtained for the problem. And the feasible solution for the example case is illustrated in Figure 5.

4.2 Heuristic based on "Route First, Split Second"

In the heuristic based on " Route First, Split Second ", a giant drone route for inspecting all the powerlines is firstly found without taking into account the endurance limitations of the drone. Then the giant drone route is split into sub-solutions to satisfy the constraints of the drone's endurance capacity and the time relationship between the ground vehicle and drone. Since the sub-solutions have been sorted before, a vehicle route is immediately formed after the splitting process.

4.2.1 Generating a giant drone route

Without considering the endurance constraint of drone, a giant drone route covering all the powerlines is generated through referring to the idea of CW Saving algorithm [36]. After dividing the powerline network into multiple segments and getting the number of powerline segments (Line 1), the first segment would be initialized as the array for recording the visiting order of segments (Line 2). Then the remaining segments would be inserted into the array in the labeled order (Line 3). Each segment would be attempted to insert into every position in the array, and the corresponding add cost would be calculated (Line 4-6). Specifically, for the segment < i, j > (i, j $\in$ VD), the forward insertion (from i to j) and reverse insertion (from j to i) would both be considered due to the undirected segment. Then the segment would be put into the array with the position of minimum adding cost and the corresponding inspection direction (Line 7). At last, a giant drone route is found. The drone route for the example case is shown in Figure 6, which is {7, a, c, b, c, d, e, f, 8}. And the main procedure is shown in Algorithm 4.

Algorithm 4: Generating a giant drone route

1 *n*: the number of transmission line segments
2 **INITIALIZE** routeArray
3 **FOR** tempSegment = 2 to *n* **DO**
4 **FOR** *i* = 1 to length(routeArray)+1 **DO**
5 Calculate added cost when inserting tempSegment into routeArray at position *i*
6 **END FOR**
7 Choose the position with minimum add cost to insert tempSegment
8 Update the routeArray
9 **END FOR**

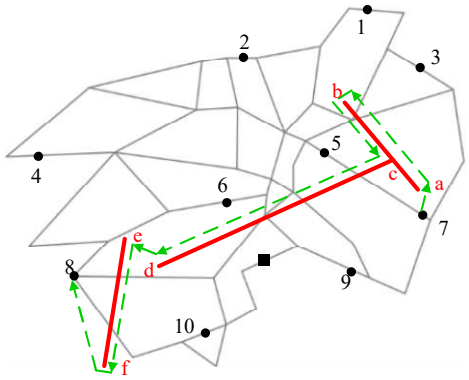

Figure 6. An illustration of the feasible solution by RFSS for the example case

4.2.2 Splitting into feasible sub-solutions

After generating a giant drone route by Algorithm 4, an interval would be applied to split the giant drone route into multiple feasible sub-solutions. Considering the flight distance between the powerline network and road network, the splitting interval is initialized as eight tenths of the maximum endurance of the drone (Line 2). Then a segment of the fixed length (the interval) would be cut from the giant drone route (Line 4). Since the inspection direction of segment has been determined, the nearest parking node to the start node of the segment would be selected as the launching node while the nearest parking node to the end node of the segment would be chosen as the taking-off node (Line 5). At this time, the feasibility of the drone route

Preprints (www.preprints.org) | NOT PEER-REVIEWED | Posted: 7 February 2019 doi:10.20944/preprints201902.0072.v1

Peer-reviewed version available at energies 2019, 12, 1385; doi:10.3390/en12071385

would be verified with the endurance constraint of the drone and the time relationship between vehicle and drone (Line 6). If it is feasible, the drone route would be constructed, which also forms a sub-solution (Line 7). If not, the value of the interval would be reduced until the sub-solution can be constructed (Line 11). After the splitting process, all sub-solutions are generated and the order of the sub-solutions is also fixed, which determines the vehicle route and can be used to quickly generate a solution for the problem.

Algorithm 5: Splitting

```
1   WHILE (the giant drone route has not been split into sub-solutions) DO
2       INITIALIZE interval = 0.8 * D / k
3       WHILE (1) DO
4           Cut the giant drone route to get a segment with the length of interval
5           Find two nearest road nodes as launching node and taking-off node
6           IF drone route can be built without violating the constraints THEN
7               Construct the drone route and get a sub-solution
8               Update the giant drone route
9               BREAK
10          ELSE
11              interval = interval - 0.1 * D / k
12          END IF
13      END WHILE
14  END FOR
```

The feasible solution obtained by RFSS is displayed in Figure 7. The splitting nodes g and h are selected, which are not the middle nodes of the segment. Then three sub-solutions are built as {7, a, c, b, c, g, 5}, {5, g, h, 6} and {6, h, d, e, f, 8}, which also generate the vehicle route as 7-5-6-8.

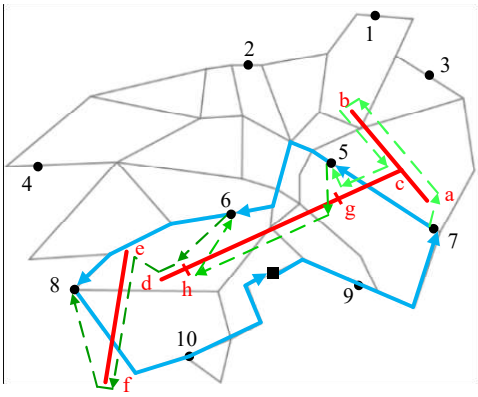

Figure 7. An illustration of the giant drone route for the example case

4.3 Local search improvement

In this section, local search is introduced to improve the feasible solution given by the constructive heuristics (CFRS or RFSS). The framework of local search is displayed in the pseudo-code of Algorithm 6.

Given a feasible solution obtained by CFRS or RFSS as an initial solution, s, (Line 1), the neighborhood list would be first initialized (Line 4). Then the neighborhood list would be explored exhaustively every time, which returns the best improvement s' (Line 4). The current solution s would be replaced with s' if s' is better (Line 6), which would reinitialize the neighborhood list (Line 7) and restart the counter k (Line 8). If all the neighborhoods in the list has been run without improvement for a determined number of times, the local search would be ended. The neighborhoods used in this part are detailed in sections 4.3.1 to 4.3.3.

Algorithm 6: Local search

```
1   s: the initial solution given by the constructive heuristic
2   k = 1
3   WHILE k ≤ N DO
4       Find the best neighbor s' ∈ N(s)
5       IF s' < s THEN
6           s ← s'
7           Reinitialize N
8           k = 1
9       ELSE
10          k = k + 1
11      END IF
12  END WHILE
```

Combined with the local search, two heuristics CFRS and RFSS can generate two hybrid algorithms, noted as CFRS-LS and RFSS-LS respectively.

4.3.1 Neighborhood 1: exchanging sub-solutions

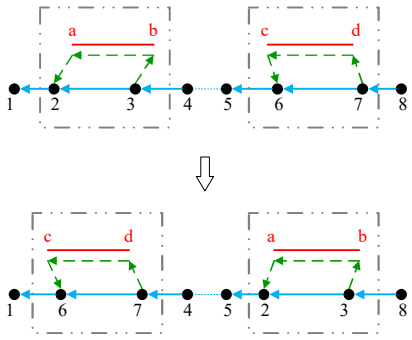

Figure 8. An illustration of exchanging sub-solutions

This neighborhood is set to exchange two sub-solutions, such as sub-solutions {2, a, b, 3} and {6, c, d, 7} in Figure 8. Since the operation has nothing to do with the drone flights inside the sub-solutions, thus only the length of the vehicle route would be changed, which is always feasible with incapacitated endurance of the vehicle. Specifically, the visiting direction of the sub-solutions can be changed, which causes four conditions due to the different vehicle routes. Only one condition is displayed in Figure 8 as the vehicle route is {1-6-7-4⋯5-2-3-8} while the route can also be changed as {1-7-6-4⋯5-2-3-8, 1-6-7-4⋯5-3-2-8}, and {1-7-6-4⋯5-3-2-8}, among which the best way of exchanging would be selected to decrease the task completing time the most.

Preprints (www.preprints.org) | NOT PEER-REVIEWED | Posted: 7 February 2019 doi:10.20944/preprints201902.0072.v1

Peer-reviewed version available at energies 2019, 12, 1385; doi:10.3390/en12071385

4.3.2 Neighborhood 2: exchanging powerline segments

This neighborhood relocates two powerline segments in two flight paths. In Figure 9, the powerline segments <c, d> and <e, f> are exchanged to check whether the task completing time can be decreased. To be specific, there are four exchange ways with different inspection directions of the two wire segments. Figure 9 illustrates an example of the operation for Neighborhood 2, where segments <c, d> and <e, f> are exchanged, and two new sub-solutions, {1, a, b, e, f, 2} and {3, c, d, 4}, are generated. In each operation, the feasibility would be verified through checking the drone's endurance and the cooperative with the ground vehicle. Only when all constraints are satisfied, the objective value of the new solution can be calculated.

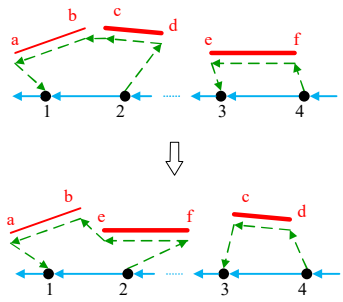

Figure 9. An illustration of exchanging powerline segments

4.3.3 Neighborhood 3: splitting powerline segments

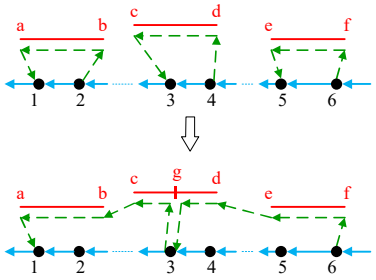

Figure 10. An illustration of splitting powerline segments

This neighborhood split a powerline segment into two new segments through the bisection method. Then it would be attempted to insert the new ones into other two sub-solutions under the constraints for the drone and the vehicle, which can improve the utilization of the drone's endurance. Correspondingly, the vehicle node for launching or recycling the drone is adjusted according to the node that the drone flies to the powerline segment. For instance, the segment <c, d> is split into segments <c, g> and <g, d> in Figure 10, which are inserted into respectively the original sub-solutions {1, a, b, 2} and {5, e, f, 6}. After adjusting the vehicle node, the new sub-solutions are presented as {1, a, b, c, g, 3} and {3, g, d, e, f, 6}.

5. Case Study and Results

In this section, a case based on the road network and the powerline network in Ji'an, a city in China, is presented. Computational experiments are conducted to compare the proposed algorithms and obtain managerial insight.

5.1 Case description

The power grid network includes three size of high-voltage powerlines (550KV, 220KV and 110KV) in Ji'an, which is shown in Figure 11(a). Since the sensors on the drone scans one area at a time, which means servel lines that are very close to each other can be inspected at the same time, thus the actual power grid is decribed as a network with mutiple arcs.

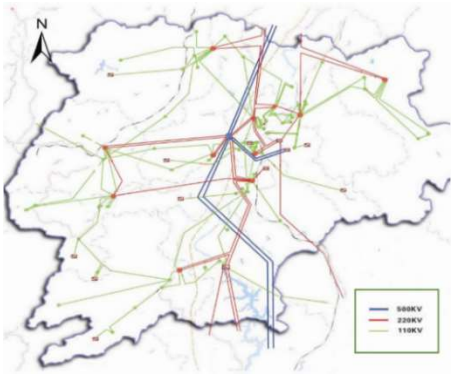

(a) the power grid in Ji'an

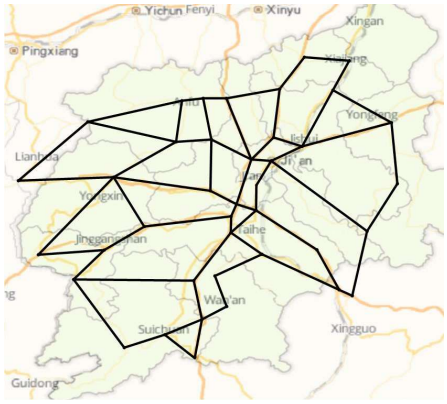

(b) the road network in Ji'an

Figure 11. The powerline network and the road network in Ji'an

The road network is built based on the main roads of Ji'an from the online map. There are 40 crossings in the road network, and the actual roads among the crossings are marked with black lines in Figure 11(b). Specifically, the latitude and longitude coordinates of the crossings are obtained from the Baidu map. A tool provided by Baidu is applied for the distance calculation of the actual roads, generating the initial distance matrix. Then the crossing distance marix is filled by the Floyd algorithm to acqure the shortest distance between any two crossings based on the road network.

Three instances with different scales of powerline networks are designed in the experiment. Six arcs of the 550KV powerlines are combined with the road netowrk, which is formed the small-scale case and illustrated in Figure 12(a). The powerlines are represented by red lines

Preprints (www.preprints.org) | NOT PEER-REVIEWED | Posted: 7 February 2019 doi:10.20944/preprints201902.0072.v1

Peer-reviewed version available at energies 2019, 12, 1385; doi:10.3390/en12071385

in Figure 12(a) while the black lines represent the road network. The dots indicate all the road parking nodes, and the black square represents the depot. Similarly, 220KV powerlines (red line) and 110KV powerlines (green line) are used for the medium-scale case and the large-scale case respectively, which are presented in Figure 12 (b) and (c). The details for three transmission lines is displayed in Table 1.

Table 1. Detail settings for the three instances

Powerline network			Road network
Electric voltage (KV)	Total length (km)	Number of arcs	Number of parking nodes
550	178.05	6	20
220	522.71	25	40
110	1228.29	71	100

(a) The small instance based on 550KV powerlines

(b) The medium-scale instance based on 220KV powerlines

(c) The large-scale instance based on 110KV powerlines

Figure 12. Three instances based on powerline network and road network in Ji'an

For the parameters related with the vehicle and drone, their values are set according to typical ones in practical application, which is shown in Table 2.

Table 2. The Parameters of vehicle and Drone

vehicle	speed	60km/h
Drone	general flying speed	50 km/h
	inspection speed	25 km/h
	capacity of battery	5000mAh
	rate of work for the sensors	200W
	coefficient φ	0.05

5.2 Experiment results and analysis

5.2.1 Experiment results

To compare the performance of the proposed algorithms, two constructive heuristics CFRS and RFSS, as well as two hybrid algorithms CFRS-LS and RFSS-LS, are all applied to solve the above three instances. In addition, the impact of the local search can also be demonstrated through the comparison between the results given by CFRS and CFRS-LS, or RFSS and RFSS-LS.

Table 3 presents the computational results for the three instances. For the small-scale and medium-scale instances, the results given by CFRS are more optimal than those by RFSS. For the large-scale instance, RFSS performs better than CFRS. There is no significant difference on the computational time of the two constructive heuristics. In addition, the local search can efficiently improve the initial solutions obtained by constructive heuristics. Take the large-scale instance as an example, after the operations of local search, the objective value decreases from 63.06 to 56.11 for CFRS and from 62.04 to 55.06 for RFSS, which respectively achieves 11.02% and 11.25% reduction on the completing time. The computational time for small-scale and medium-scale instances is controlled in 2 seconds while the process solving the large-scale instance consumes about 5 seconds.

Preprints (www.preprints.org) | NOT PEER-REVIEWED | Posted: 7 February 2019 doi:10.20944/preprints201902.0072.v1

Peer-reviewed version available at energies 2019, 12, 1385; doi:10.3390/en12071385

Table 3. Results of the three instances by different algorithms

case	Objective value (h)				Computational time (s)			
	CFRS	RFSS	CFRS-LS	RFSS-LS	CFRS	RFSS	CFRS-LS	RFSS-LS
small	9.97	10.83	9.58	9.56	0.13	0.16	1.22	1.36
medium	26.91	28.32	24.66	24.03	0.45	0.50	1.52	1.68
large	63.06	62.04	56.11	55.06	1.23	1.30	4.33	5.19

Table 4. Sensitivity results for different inspection speeds and battery powers

Battery power (mAh) \ Inspection speed (km/h)	5	10	15	20	25	30	35	40
2000	111.05	60.77	43.20	35.84	32.30	27.21	24.94	23.56
3000	107.31	57.73	41.36	32.50	29.75	24.64	22.36	20.84
4000	102.98	55.63	38.91	30.12	26.78	22.53	20.29	18.69
5000	100.41	53.22	36.98	28.59	24.03	20.77	18.50	16.80
6000	99.40	52.06	35.47	27.51	22.86	19.47	17.20	15.50
7000	98.88	51.15	34.25	26.96	22.29	18.21	16.31	14.29
8000	98.33	50.67	33.69	26.62	21.86	17.80	15.52	13.82

5.2.2 Sensitivity analysis

Two critical parameters related to the performance of the drone are considered in the sensitivity analysis, which are the inspection speed and the capacity of battery power. The flying speed of the drone during its inspection of the powerline is mainly constrained by the performance of the inspection sensor carried by the drone and the capability of the software system for inspection data analysis. Technical improvement on these hardware and software can improve the inspection speed of the drone. The capacity of the battery power constrains the endurance of the drone in each flying route. Thus, both two parameters are critical in the investigated problem, and sensitivity analysis on these parameters can help us observe their impact on the efficiency of the whole cooperated inspection system. The medium-scale instance is used in the sensitivity analysis, and the best objective values of four algorithms are reported in Table 4.

(1) Impact analysis of the inspection speed

For analyzing the impact of the inspection speed, we vary its value from 5 km/h to 40 km/h, and calculate the coverall completing time under different inspection speeds. From the computational results in Table 4, it can be seen that the overall completing time decreases as the inspection speed increases. To further analyze the effect of this parameter, the detail experiment results with the battery power of 5000 mAh and different inspection speeds from 5 to 40 km/h are reported in Figure 13. The exact results are also presented in Table 5.

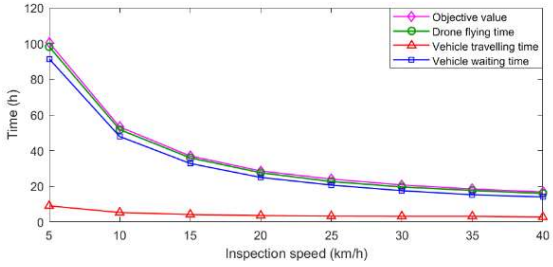

Figure 13. Computational results under different inspection speeds

As the inspection speed increases from 5km/h to 20km/h, the overall completing time shows a significant reduction from 100.41h to 28.59h. When the inspection speed is over 20km/h, the completing time decreases slowly as the inspection speed increases. The flight time of the drone, the travelling time and waiting time of the vehicle is also presented. The varying of the flight time of the drone and the waiting time of the vehicle is similar to that of the overall completing time. The absolute reduction of the vehicle's travelling time is not significant, which is from 9.06h to 2.28h, but its relative reduction is great. In all, the improvement of inspection speed can effectively reduce the overall completing time.

(2) Impact analysis of the battery capacity

To investigate the effects of the drone's battery

Preprints (www.preprints.org) | NOT PEER-REVIEWED | Posted: 7 February 2019 doi:10.20944/preprints201902.0072.v1

Peer-reviewed version available at energies 2019, 12, 1385; doi:10.3390/en12071385

capacity,

Table 5. Results for different inspection speeds under fixed battery of 5000 mAh

Inspection speed	5	10	15	20	25	30	35	40
Objective	100.41	53.22	36.98	28.59	24.03	20.77	18.50	16.80
Drone flying time	98.15	51.74	35.94	27.60	22.68	19.64	17.66	16.00
vehicle Travelling time	9.06	5.34	4.20	3.62	3.33	3.24	3.23	2.80
vehicle Waiting time	91.35	47.88	32.78	24.97	20.70	17.54	15.27	14.00

Table 6. Results for different battery powers under fixed inspection speed of 25km/h

Battery power	2000	3000	4000	5000	6000	7000	8000
Objective	32.30	29.75	26.78	24.03	22.86	22.29	21.86
Drone flying time	29.84	28.23	25.50	22.68	21.45	20.68	20.46
Vehicle travelling time	7.77	6.27	4.75	3.33	3.21	3.13	2.86
Vehicle waiting time	24.53	23.38	22.03	20.70	19.65	19.26	19.00

the detailed results for the battery power varying from 2000 to 8000mAh is analyzed, while the inspection speed is fixed at 25 km/h. The results are reported in Table 6 and compared in Figure 14.

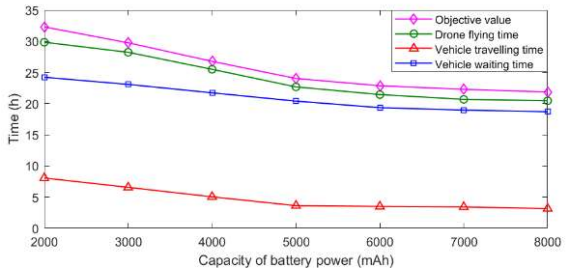

Figure 14. Computational results under different battery powers

As Figure 14 displays, the objective value, that is the overall completing time, decreases with the increasing of the battery capacity. Similar trends are also observed for the drone's flying time, the vehicle's travelling time and waiting time. Because higher battery capacity enables the drone flying more longer distance in each sub-solution route, the vehicle would stop less times for launching and recycling of the drone, which causes a higher utilization of the drone endurance on powerline inspection. The flatter curve in Figure 14 indicates that it does work on improving the efficiency by increasing the drone's battery capacity, but its influence is lower compared to that of the inspection speed as shown in Figure 13.

6. Conclusion

In this paper, recognizing that the cooperation of the ground vehicle and the drone can significantly improve the efficiency of high-voltage powerline inspection, the novel powerline inspection system is investigated. When the vehicle travels on the road network while the drone flies along the high-voltage power transmission line, a new variant of routing problem is generated for simultaneously optimizing the routes for the vehicle and the drone, which integrates the classical Travelling Salesman Problem and Arc Routing problem. To solve the problem, two constructive heuristics based on CFRS and RFSS are designed. Also, the local search with three neighborhood operators is proposed to improve the quality of the solution obtained by CFRS and RFSS.

Different-scale cases based on the road network and the high-voltage powerline network of Ji'an are designed to test the performance of the proposed algorithms. Furthermore, two factors are considered in sensitivity tests, which are the drone's inspection speed and battery capacity. Experimental results indicate that proper improvement on technologies for improving the inspection speed or enlarging the capacities of the drone endurance would be helpful to shorten the overall completing time of the powerline inspection. In addition, technical improvement on the inspection speed is more important than that on the battery capacity.

In the investigated system, it is assumed that the vehicle can only carry one drone. A meaningful future research is to study the system involving multiple drones, which would be more important for large scale networks. New algorithms also have to be developed for optimizing the routes for multiple drones and their vehicle.

Acknowledgments

The research is supported by the National Natural Science Foundation of China (grant nos. 71771215 and 71471175) and the Natural Science Fund for Distinguished

Young Scholars of Hunan Province (2018JJ1035).

References

[1] West, L. M., & Segerstrom, T. (2000, March). Commercial applications in aerial thermography: power line inspection, research, and environmental studies. In *Thermosense XXII*(Vol. 4020, pp. 382-387). International Society for Optics and Photonics.

[2] Jiang, S., Jiang, W., Huang, W., & Yang, L. (2017). UAV-based oblique photogrammetry for outdoor data acquisition and offsite visual inspection of transmission line. *Remote Sensing*, *9*(3), 278.

[3] https://aithority.com/robots/autonomous-vehicles/drones/ameren-successfully-completes-industry-leading-60-mile-drone-flight-over-transmission-lines-paving-the-way-for-safe-efficient-aerial-infrastructure-inspections/

[4] http://kokomoperspective.com/politics/indiana/i-m-using-drones-to-inspect-randolph-county-transmission-lines/article_4f36f473-8539-5aa3-8f47-aac7dccf3883.html

[5] Deng, C., Wang, S., Huang, Z., Tan, Z., & Liu, J. (2014). Unmanned aerial vehicles for power line inspection: A cooperative way in platforms and communications. *J. Commun*, *9*(9), 687-692.

[6] Wu, F. F., Zheng, F. L., & Wen, F. S. (2006). Transmission investment and expansion planning in a restructured electricity market. *Energy, 31*(6-7), 954-966.

[7] Niemi, R., & Lund, P. D. (2010). Decentralized electricity system sizing and placement in distribution networks. *Applied Energy, 87*(6), 1865-1869.

[8] Fürsch, M., Hagspiel, S., Jägemann, C., Nagl, S., Lindenberger, D., & Tröster, E. (2013). The role of grid extensions in a cost-efficient transformation of the European electricity system until 2050. *Applied Energy*, *104*, 642-652.

[9] Guerra, O. J., Tejada, D. A., & Reklaitis, G. V. (2016). An optimization framework for the integrated planning of generation and transmission expansion in interconnected power systems. *Applied Energy*, *170*, 1-21.

[10] Sarıca, K., Kumbaroğlu, G., & Or, I. (2012). Modeling and analysis of a decentralized electricity market: An integrated simulation/optimization approach. *Energy, 44*(1), 830-852.

[11] Sawada, J., Kusumoto, K., Maikawa, Y., Munakata, T., & Ishikawa, Y. (1991). A mobile robot for inspection of power transmission lines. *IEEE Transactions on Power Delivery*, *6*(1), 309-315.

[12] Zhou, F. Y., Wang, J. D., Li, Y. B., Wang, J., & Xiao, H. R. (2005, August). Control of an inspection robot for 110KV power transmission lines based on expert system design methods. In *Control Applications, 2005. CCA 2005. Proceedings of 2005 IEEE Conference on* (pp. 1563-1568). IEEE.

[13] Zhu, X., Zhou, J., Wang, H., Fang, L., & Zhao, M. (2006, December). An autonomous obstacles negotiating inspection robot for extra-high voltage power transmission lines. In *2006 9th International Conference on Control, Automation, Robotics and Vision* (pp. 1-6). ieee.

[14] Katrasnik, J., Pernus, F., & Likar, B. (2010). A survey of mobile robots for distribution power line inspection. *IEEE Transactions on Power Delivery*, *25*(1), 485-493.

[15] Guo, J., Wu, G., Liu, B., Wang, Q., Wang, Z., Ma, Y., ... & Liu, B. (2009, March). Database environment of an inspection robot for power transmission lines. In *Power and Energy Engineering Conference, 2009. APPEEC 2009. Asia-Pacific* (pp. 1-4). IEEE.

[16] Grauman, K., & Darrell, T. (2006, June). Unsupervised learning of categories from sets of partially matching image features. In *Computer Vision and Pattern Recognition, 2006 IEEE Computer Society Conference on* (Vol. 1, pp. 19-25). IEEE.

[17] Besada, J. A., Bergesio, L., Campaña, I., Vaquero-Melchor, D., López-Araquistain, J., Bernardos, A. M., & Casar, J. R. (2018). Drone Mission Definition and Implementation for Automated Infrastructure Inspection Using Airborne Sensors. *Sensors*, *18*(4), 1170.

[18] Seo, J., Duque, L., & Wacker, J. (2018). Drone-enabled bridge inspection methodology and application. *Automation in Construction*, *94*, 112-126.

[19] Moore, A., Schubert, M., & Rymer, N. (2018). Autonomous Inspection of Electrical Transmission Structures with Airborne UV Sensors and Automated Air Traffic Management. In *2018 AIAA Information Systems-AIAA Infotech@ Aerospace* (p. 1628).

[20] Morita, M., Kinjo, H., & Sato, S. (2017, November). Autonomous flight drone for infrastructure (transmission line) inspection (3). In *Intelligent Informatics and Biomedical Sciences (ICIIBMS), 2017 International Conference on* (pp. 198-201). IEEE.

[21] Hrabar, S., Merz, T., & Frousheger, D. (2010, October). Development of an autonomous helicopter for aerial powerline inspections. In *Applied Robotics for the Power Industry (CARPI), 2010 1st International Conference on*(pp. 1-6). IEEE.

[22] Luque-Vega, L. F., Castillo-Toledo, B., Loukianov, A., & Gonzalez-Jimenez, L. E. (2014, April). Power line inspection via an unmanned aerial system based on the quadrotor helicopter. In *MELECON 2014-2014 17th IEEE Mediterranean Electrotechnical Conference* (pp. 393-397). IEEE.

[23] Huang, S. , Gu, X. , & Zhang, J. . (2014). Design of new oil moving fixed-wing unmanned aerial vehicle for power line patrolling. *Automation of Electric Power Systems, 38*(4), 104-108+126.

[24] Xie, X., Liu, Z., Xu, C., & Zhang, Y. (2017). A Multiple Sensors Platform Method for Power Line Inspection Based on a Large Unmanned Helicopter. *Sensors*, *17*(6), 1222.

[25] Pirbodaghi, S., Thangarajan, D., Liang, T. H., Shanmugavel, M., Ragavan, V., & Sequeira, J. S. (2015, December). A cooperative heterogeneous Unmanned Autonomous Systems solution for monitoring and inspecting power distribution system. In *Control, Instrumentation, Communication and Computational Technologies (ICCICCT), 2015 International Conference on* (pp. 495-502). IEEE.

[26] Sampedro, C., Martinez, C., Chauhan, A., & Campoy, P. (2014, July). A supervised approach to electric tower detection and classification for power line inspection. In *Neural Networks (IJCNN), 2014 International Joint Conference on* (pp. 1970-1977). IEEE.

[27] Li, B., & Chen, C. (2018). Transmission line detection based on a hierarchical and contextual model for aerial images. *Journal of Electronic Imaging*, *27*(4), 043054.

[28] Santos, T., Moreira, M., Almeida, J., Dias, A., Martins, A., Dinis, J., ... & Silva, E. (2017, April). PLineD: Vision-based power lines detection for Unmanned Aerial Vehicles. In *Autonomous Robot Systems and Competitions (ICARSC), 2017 IEEE International Conference on* (pp. 253-259). IEEE.

[29] Martinez, C., Sampedro, C., Chauhan, A., & Campoy, P. (2014, May). Towards autonomous detection and tracking of electric towers for aerial power line inspection. In *Unmanned Aircraft Systems*

(ICUAS), 2014 International Conference on (pp. 284-295). IEEE.

[30] Zhang, F., Wang, W., Zhao, Y., Li, P., Lin, Q., & Jiang, L. (2016, October). Automatic diagnosis system of transmission line abnormalities and defects based on UAV. In *Applied Robotics for the Power Industry (CARPI), 2016 4th International Conference on* (pp. 1-5). IEEE.

[31] Vaquero-Melchor, D., Campaña, I., Bernardos, A. M., Bergesio, L., & Besada, J. A. (2018, June). A Distributed Drone-Oriented Architecture for In-Flight Object Detection. In *International Conference on Hybrid Artificial Intelligence Systems* (pp. 433-445). Springer, Cham.

[32] La Cour-Harbo, A. (2017, June). Quantifying risk of ground impact fatalities of power line inspection BVLOS flight with small unmanned aircraft. In *Unmanned Aircraft Systems (ICUAS), 2017 International Conference on* (pp. 1352-1360). IEEE.

[33] Liu, C. A., Wang, L., & Liu, C. (2009). Mission planning of the flying robot for powerline inspection. *Progress in Natural Science*, *19*(10), 1357-1363.

[34] Baik, H., & Valenzuela, J. (2018). Unmanned Aircraft System Path Planning for Visually Inspecting Electric Transmission Towers. *Journal of Intelligent & Robotic Systems*, 1-15.

[35] D'Andrea, R. (2014). Guest editorial can drones deliver?. *IEEE Transactions on Automation Science and Engineering*, *11*(3), 647-648.

[36] Clarke, G., & Wright, J. W. (1964). Scheduling of vehicles from a central depot to a number of delivery points. *Operations research*, *12*(4), 568-581.